Conformational Modulation of Human Cytochrome P450 2E1 by Ethanol and Other Substrates: A CO Flash Photolysis Study

Stanley V. Smith,‡ Aditya P. Koley,‡ Renke Dai,‡ Richard C. Robinson,‡ Hoyee Leong,‡ Allen Markowitz,§ and Fred K. Friedman*,‡

Laboratory of Molecular Carcinogenesis, National Cancer Institute, and Bioengineering and Physical Science Program, National Institutes of Health, Bethesda, Maryland 20892

Received January 20, 2000; Revised Manuscript Received March 7, 2000

ABSTRACT: The alcohol-inducible cytochrome P450 2E1 is a major human hepatic P450 which metabolizes a broad array of endogenous and exogenous compounds, including ethanol, low-molecular weight toxins, and fatty acids. Several substrates are known to stabilize this P450 and inhibit its cellular degradation. Furthermore, ethanol is a known modulator of P450 2E1 substrate metabolism. We examined the CO binding kinetics of P450 2E1 after laser flash photolysis of the heme−CO bond, to probe the effects of ethanol and other substrates on protein conformation and dynamics. Ethanol had an effect on the two kinetic parameters that describe CO binding: it decreased the rate of CO binding, suggesting a decrease in the protein's conformational flexibility, and increased the photosensitivity, which indicates a local effect in the active site region such as strengthening of the heme−CO bond. Other substrates decreased the CO binding rate to varying degrees. Of particular interest is the effect of arachidonic acid, which abolished photodissociation in the absence of ethanol but had no effect in the presence of ethanol. These results are consistent with a model of P450 2E1 whereby arachidonic acid binds along a long hydrophobic binding pocket and blocks exit of CO from the heme region.

The cytochrome P450 superfamily is comprised of P450s[1] with unique substrate and catalytic activity profiles, which collectively catalyze the oxidation of a wide variety of xenobiotic and endogenous compounds (*1*−*5*). Numerous factors govern the expression of catalytic activity by mammalian microsomal P450s. These include interactions with the endoplasmic membrane as well as the redox partners NADPH−cytochrome P450 reductase and cytochrome b_5, which transfer electrons to P450 during the catalytic cycle. In addition to these catalytically essential functions, such interactions may also modulate P450 activity by introducing structural changes in the P450 and/or altering P450−substrate interactions. For example, the membrane lipid constitution affects the P450 spin equilibrium (*6*) and NADPH−cytochrome P450 reductase influences the mode of substrate binding to P450 (*7*). Substrate binding also structurally perturbs P450, and may thus control the uniqueness of P450-catalyzed reactions by inducing intramolecular changes that mediate and stabilize subsequent conformational changes. We previously employed the flash photolysis technique to examine the kinetics of CO binding to P450 heme iron as a probe of P450−substrate interactions (*8*−*15*). Since the kinetics reflect the rate of CO diffusion through the protein matrix to the heme iron, it is a sensitive probe of the local active site environment as well as of P450 conformation and structural dynamics. The kinetics thus yield unique information about the heme environment, protein structure and dynamics, and the mode of substrate binding. Specifically, studies with rat cytochrome P450s 2B1 (*15*) and 1A1 (*14*) and human P450s 1A1 (*10*) and 3A4 (*8*, *9*, *13*) showed that substrate binding modulates P450 conformation and dynamics and access of the ligand to the heme iron. This approach uniquely illuminated these properties of P450 3A4 and showed that this P450, which metabolizes a variety of structurally dissimilar drugs, exists in alternate conformational states with distinct substrate specificities (*8*, *13*). We furthermore showed that binding of different substrates differentially modulated the conformation of this P450. More importantly, this technique allowed us to measure these subtle properties of the protein while in a biological membrane milieu rather than in a reconstituted system which inherently involves at least partial disruption of the native state of the protein.

We sought to apply a similar approach to address certain outstanding questions in human cytochrome P450 2E1 (*16*−*20*). This xenobiotic-metabolizing human hepatic P450 metabolizes a variety of small lipophilic toxins, and some metabolites have been linked to human cancers. Among the substrates of this P450 are the drug acetaminophen (*21*) and arachidonic acid (*22*). A clinically significant property of P450 2E1 is its inducibility by ethanol, which is also a substrate. This inducibility introduces a variety of other concerns such as alcohol−drug interactions (*16*), efficacy of drug treatments, and hepatotoxicity which is derived from generation of free radicals during the catalytic cycle (*20*).

* To whom correspondence should be addressed: NIH, Bldg. 37, Room 3E-24, Bethesda, MD 20892. Telephone: (301) 496-6365. Fax: (301) 496-8419. E-mail: fkfried@helix.nih.gov.

‡ Laboratory of Molecular Carcinogenesis, National Cancer Institute.

§ Bioengineering and Physical Science Program, National Institutes of Health.

[1] Abbreviations: P450, cytochrome P450; EtOH, ethanol; PBS, 10 mM potassium phosphate and 0.1 M NaCl (pH 7.4).

10.1021/bi000129l
Published on Web 04/21/2000

The hepatotoxicity is observed since this P450 is more prone to production of destructive free radicals than other P450s (*23*). The stability and reactivity of P450 2E1 are thought to play a role in the manifestations of these conditions as the presence of certain substrates and ligands stabilizes the protein (*17, 24*). These observations on the structure−function mechanism of P450 2E1 reflect unique local properties of its active site as well as global properties relative to its structural dynamics. A better understanding of the structural properties of P450 2E1 and of its interactions with substrates will ultimately help elucidate the effect of alcohol as well as factors that lead to its production of toxic or carcinogenic metabolites.

To gain insight into the molecular basis for the P450 2E1 interactions with ethanol and a number of other biologically relevant substrates, we investigated their effects on human P450 2E1 conformation and dynamics. We examined these interactions by measuring both CO binding kinetics and substrate-induced spectral changes, which reflect dynamic and static properties, respectively. The experimental results were interpreted with a molecular model of P450 2E1. We found that various substrates, either alone or in combination with ethanol, exert variable effects on the CO binding kinetics of P450 2E1, and hence differentially modulate the conformation and dynamics and protein-assisted positioning of the substrate, ligand, and heme in the P450 2E1 active site. The results indicate that this P450 is more conformationally homogeneous and more flexible than the previously examined P450s (3A4 and 1A1). Most significant, the kinetics suggest that the mechanism by which ethanol stabilizes P450 2E1 is by reducing its conformational flexibility.

MATERIALS AND METHODS

Human P450 2E1. This P450 was expressed in SF9 insect cells using a recombinant baculovirus as described previously (*25*). One liter of cells was harvested by low-speed centrifugation (3000*g* for 20 min) and washed two times by suspension in PBS and subsequent centrifugation, and the washed pellet was stored at −80 °C until it was used. Frozen cells were thawed, homogenized for 10 strokes in a total volume of 60 mL of PBS per liter of original culture volume, and aliquoted into individual tubes for storage at −80 °C until they were used. The total P450 content was spectrally determined (*26*) and the protein content measured by the bicinchoninic acid method (*27*).

Difference Spectroscopy. Aliquots of P450 2E1 were thawed and diluted to a final concentration of 2 μM with 100 mM sodium phosphate (pH 7.4) and 20% glycerol (w/v). Absorbance differences were measured at 23 °C using a SLM DW2000 spectrophotomer set to split-beam mode. Identical samples were placed in the sample and reference positions of the cuvette holder. Substrates (obtained from Sigma, St. Louis, MO) from 100 mM stock solutions in water (except acetaminophen and halothane which were in methanol) were added to the sample cuvette, while an equal volume of solvent was added to the reference cuvette. After the mixture had been stirred for 2 min to ensure equilibration, a wavelength scan from 350 to 600 nm was obtained. For titrations, successive additions of substrate were made followed by equilibration and a wavelength scan. The magnitude of the difference between the absorbances of the peaks near 390 and 420 nm versus the substrate concentration was plotted, and a nonlinear least-squares fit to the Michaelis−Menten model was used to obtain the apparent spectroscopic binding constant, K_s. These calculations were carried out using Origin software (Microcal, Northampton, MA).

Spectral measurements of ethanol binding presented a unique problem since ethanol reduced the apparent absorbance throughout the wavelength range. This observation presumably is derived from an ethanol effect on the biological membrane which reduces the turbidity. Since the relationship between wavelength and the turbidity-derived absorbance is not linear but rather obeys a fourth-power law, the measured absorbance spectra must be corrected by subtracting the turbidity contribution (*28*). This was accomplished by extrapolating from the nonabsorbing higher-wavelength region of linear log absorbance versus log wavelength plots, to the Soret region to determine the true, turbidity-corrected, absorbance values. In this manner, the true absorbance, and subsequent difference spectra, were obtained.

CO Binding Kinetics. Reactions were carried out under pseudo-first-order conditions using 1.3 μM P450 2E1 (corresponding to 1.2 mg/mL cell homogenate protein) and 20 μM CO, at 23 °C in 100 mM sodium phosphate (pH 7.4) containing 20% glycerol (w/v), in a total volume of 1.0 mL. When present, substrates from 100 mM stock solutions in the buffer described above (except acetaminophen and halothane which were in methanol) were first added to yield a final concentration of 1 mM (with the exception of ethanol which yielded 50 mM), as initial experiments showed that this concentration produced maximal effects on the CO binding kinetics. Addition of methanol alone had no effect on the CO binding kinetics. The mixture was then incubated for 20 min at 23 °C prior to addition of CO and reduction with dithionite. Photodissociation of the P450−CO complex and monitoring of CO binding kinetics at 450 nm were performed as described previously (*29*). Standard exponential analysis of kinetic data was performed according to

$$\Delta A = \sum_{i=1}^{n} \Delta A_{i0} e^{-k_i t} \quad (1)$$

where ΔA is the observed absorbance change during the reaction course, ΔA_{i0} is the maximum absorbance change for kinetic component i, k_i is the observed pseudo-first-order rate constant for component i, and n is the number of independent components. When thus analyzed, all kinetic data were best described by a single exponential, for which the above equation simplifies to

$$\Delta A = \Delta A_0 e^{-kt} \quad (2)$$

Least-squares analysis was performed with RS/1 statistical analysis software (BBN Software Products, Cambridge, MA) on a Dell Pentium microcomputer.

Molecular Modeling. The P450 2E1 homology model was constructed on the basis of the crystal structure of P450 BM-3 (*30*). The program QUANTA with its Protein Design Module (Molecular Simulations Inc., San Diego, CA) was applied to generate a model by methods previously used for modeling P450s 2B1 (*31*) and 1A2 (*32*). To optimize the alignment of the human P450 2E1 sequence with that of the P450 BM-3

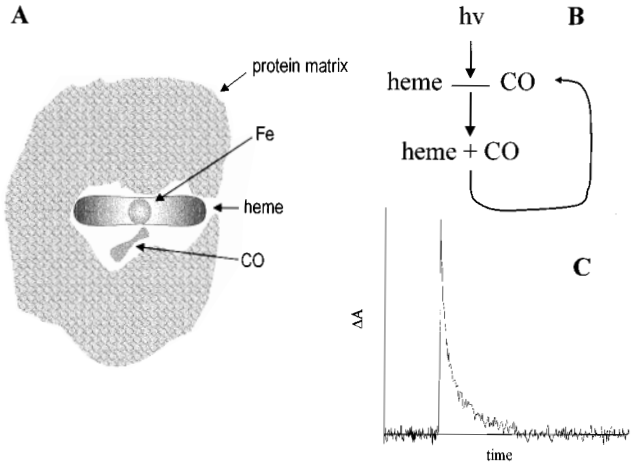

FIGURE 1: Scheme for CO flash photolysis. (A) The CO molecule is initially bound to the heme iron embedded in the P450 protein matrix. (B) This photosensitive bond is broken upon excitation with a laser flash at 530 nm. The CO diffuses out of the protein and then migrates through the protein matrix to reassociate with the heme. (C) These events are followed via the absorption changes at 450 nm. This spike represents the rapid CO dissociation, followed by a decay which reflects the reassociation reaction. Details of the instrumentation have been described previously (*29*).

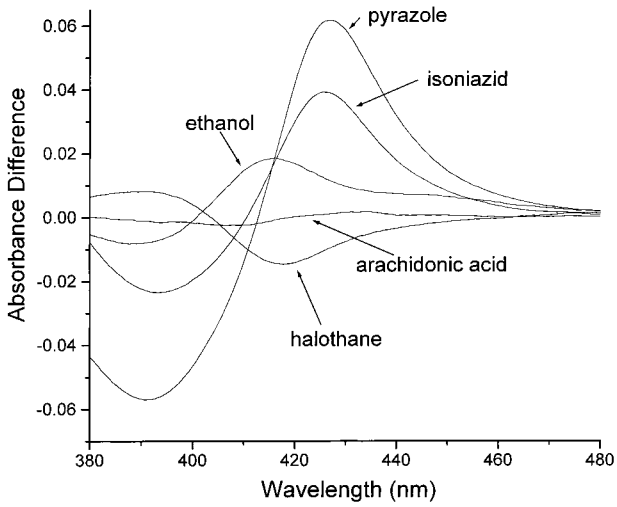

FIGURE 2: Difference spectra for P450 2E1 ligands**.** The spectral change upon addition of the indicated compounds is shown. Concentrations of all compounds were 1 mM, except for those of isoniazid (12 mM) and ethanol (500 mM).

template, multiple sequence alignments were first performed using several P450s within the P450 II subfamily (*31*). Details of the homology modeling procedure will be reported elsewhere. Since arachidonic acid is hydroxylated by P450 2E1, the QUANTA-generated P450 structure was refined after docking this substrate into the substrate binding pocket in a manner similar to the docking of palmitic acid into P450 BM-3 (*33*). The arachidonic acid structure was generated with QUANTA's Builder application, and its energy was minimized with 3000 steps of steepest descents, followed by 3000 steps of the conjugate gradient method. The adopted-basis Newton Raphson method then was applied until the energy gradient converged to a value of 0.001 kcal mol^{-1} $Å^{-1}$. The structure was further subjected to molecular dynamic refinement by heating to 600 K for 6 ps and equilibration at 600 K for 30 ps. The last 10 recorded structures (over 5 ps) were averaged and minimized, and the resulting average structure was subjected to additional molecular dynamics heating to 300 K for 6 ps and simulation at 300 K for 40 ps. The average of the last 10 recorded structures (over 5 ps) was then energy minimized to yield the final P450−arachidonic acid complex. During the dynamic equilibration and simulation, the temperature window was set at ±30 K, and the temperature checking frequency was once every five steps.

RESULTS

Flash Photolysis Method. Figure 1 depicts the basic principles of the CO flash photolysis method. The CO molecule, which is the probing ligand, is initially bound to the heme iron within the P450 protein (Figure 1A). The reaction sequence in Figure 1B shows that a pulse of laser light ($h\nu$) first disrupts the photosensitive heme−CO bond. This is followed by rapid diffusion of the CO molecule from the protein interior to the surrounding solvent and subsequent recombination with the heme. The graphical representation of this reaction (Figure 1C) shows the abrupt absorbance change at 450 nm which accompanies the photodissociation, followed by the CO recombination as the system relaxes back to the initial P450−CO complex. The decay kinetics yield information about the rate at which the CO diffuses back through the protein matrix to the heme iron. The rate of binding (k) reflects conformational dynamics as well as active site accessibility for events taking place in the protein on a rapid time scale, typically milliseconds under our experimental setup. The amplitude of the absorbance peak (ΔA_0) reflects the strength and photolability of the heme−CO bond and is sensitive to changes in the local environment of the heme active site. The two parameters, k and ΔA_0, thus yield unique and complementary information about the protein structure and dynamics and active site of the P450, and are sensitive to perturbations introduced by added substrate.

Binding of Substrates to P450 2E1. Representative substrates were selected on the basis of their known metabolism by P450 2E1, and importance in drug-mediated toxicity or physiological pathways. Ethanol is a substrate, inducer, and stabilizer of P450 2E1. The drugs halothane and acetaminophen, and arachidonic acid, a mediator of numerous physiological processes, are P450 2E1 substrates. Pyrazole and isoniazid are inducers as well as substrates of P450 2E1 (*20*).

The static difference spectra for the P450 2E1 ligands used in this study are shown in Figure 2. Spectral changes in the Soret region reflect shifts in the electronic state of the heme, including the low-spin−high-spin equilibrium, and are sensitive to binding of axial ligands such as water (*34*). In the absence of substrate, the human P450 2E1 spectrum revealed a mixture of spin states, with a peak at 412 nm (corresponding to low spin) and a shoulder at 394 nm (corresponding to high spin), at an absorbance ratio of 1:0.88 (data not shown). A mixed spin state for this P450 has also previously been reported (*35*). Halothane binds P450 2E1 with a K_s of 0.22 mM (Table 1), yielding a type I difference spectrum. This spectral change is typical for a binding mode that displaces bound water from the heme and shifts the iron spin state toward high spin. Pyrazole and isoniazid (K_s = 11 μM and 4 mM, respectively) yield type II difference spectra, indicating that they replace the water ligand and perturb the heme iron toward the low-spin state. Ethanol, which both induces P450 2E1 and stabilizes it at the protein level, binds with a

Table 1: Equilibrium and Kinetic Parameters for P450 2E1 Interactions[a]

addition	K_s (mM)	binding mode	k (s^{-1})	ΔA_0
none			578 ± 63	0.0092 ± 0.0015
ethanol	167	reverse type I	270 ± 19	0.0111 ± 0.0014
halothane	0.223	type I	6.7 ± 0.9	0.0227 ± 0.0030
isoniazid	4.3	type II	354 ± 71	0.0078 ± 0.0013
pyrazole	0.011	type II	534 ± 117	0.0085 ± 0.0028
acetaminophen	ns[b]	ns	386 ± 17	0.0082 ± 0.0015
arachidonic acid	ns	ns	nd[c]	nd

[a] The spectral dissociation constant K_s was determined from the magnitude of the difference spectra upon titration of 2 μM P450 2E1 with the indicated substrate. The pseudo-first-order rate constant for CO binding (k) and the absorbance of photodissociated CO (ΔA_0) were obtained from kinetic progress curves in the absence and presence of 1 mM substrate (50 mM for ethanol). [b] No spectral change was detected. [c] Not determined since no CO photodissociation was observed.

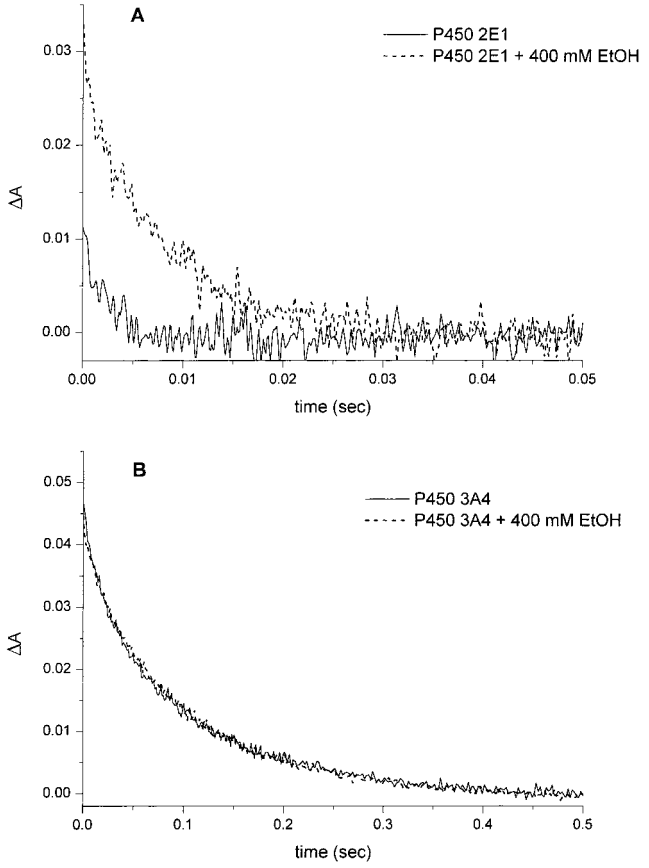

FIGURE 3: Effects of ethanol on P450 2E1 CO binding kinetics. (A) The time course of CO binding is shown for 1.3 μM P450 2E1 in the absence or presence of 400 mM ethanol. (B) Corresponding kinetic traces for CO binding to P450 3A4.

K_s of 167 mM, yielding a difference spectrum with reverse type I properties. Addition of arachidonic acid or acetaminophen showed no measurable difference spectra. Since these are P450 2E1 substrates, they obviously bind the protein, but the absence of a spectral perturbation shows that their mode of binding does not displace the heme water ligand.

Effects of Ethanol on the Kinetics of CO Binding to P450 2E1. Kinetic profiles for CO binding to P450 2E1 in the absence and presence of 400 mM ethanol are illustrated in Figure 3A. As a control, the corresponding kinetic traces were measured for P450 3A4 (Figure 3B). The results first

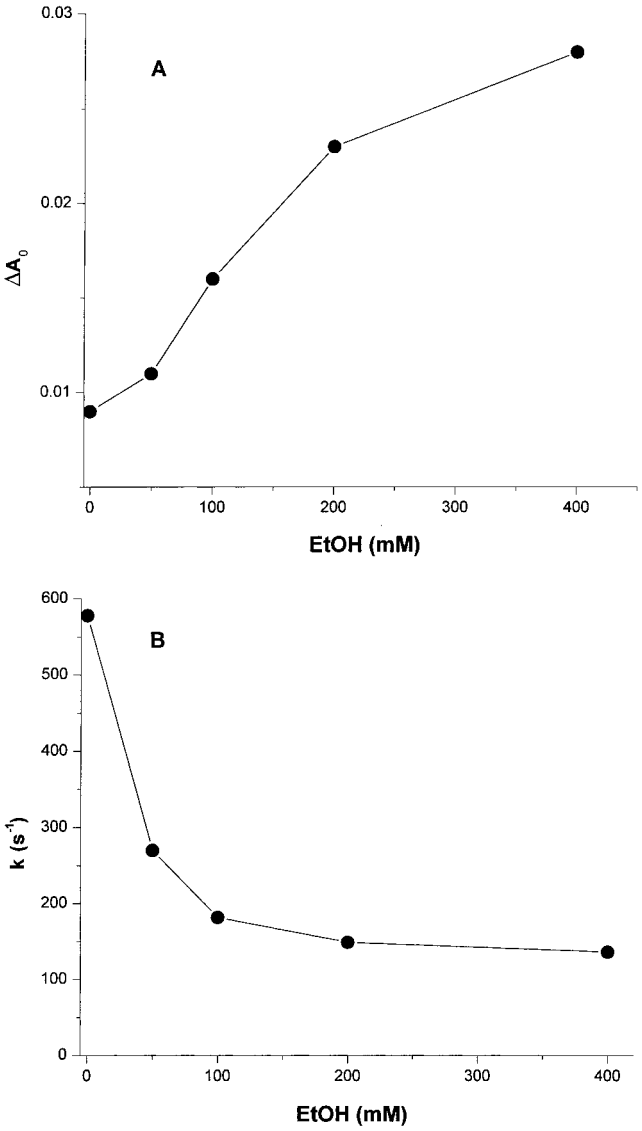

FIGURE 4: Ethanol effect on the CO binding kinetic parameters of P450 2E1. (A) Effect of ethanol concentration on the photodissociation as reflected by ΔA_0. (B) Effect of ethanol on the CO binding rate as reflected by k. The P450 2E1 concentration was 1.3 μM.

show that ethanol affects the kinetics of P450 2E1 but not 3A4. The P450 2E1 kinetics are well described by a single exponential at several ethanol concentrations (Figure 4), and yield values for k, the apparent rate constant of CO binding, and ΔA_0, the photosensitivity parameter. The results without ethanol show that the CO binding rate of P450 2E1 was 578 s^{-1}, a value greater than that of the previously examined P450s, 2B1 (*15*), 1A1 (*9*, *14*), and 3A4 (*8*). The rate reflects the ease of CO diffusion from solvent through the protein matrix to the heme, and its value depends on the conformational flexibility of the P450. This higher rate for P450 2E1 thus suggests a very accommodating path to the active site, relative to that of the other P450s.

The dependencies of the kinetic parameters on ethanol concentration are shown in Figure 4. At the highest concentration that was tested (400 mM), ethanol dramatically decreased the rate from 578 to 136 s^{-1}, a decrease of 76%. This reduced rate of CO migration from solvent to the interior heme shows a decrease in the mobility or dynamic fluctuations of the P450 molecule, which is consistent with the

reported stabilization of this P450 by ethanol (*36*). Although the mechanism of stabilization is unknown, our results suggest the ethanol-induced P450 rigidity may be a factor, since rigidity reduces susceptibility to proteolytic degradation (*37*).

The ΔA_0 parameter gauges the ease of CO photodissociation from P450, which depends on the both the photosensitivity of the heme−CO bond and the ease of egress of photodissociated CO from the protein interior. Compared to the previously studied P450s which undergo essentially complete photodissociaton, P450 2E1 in the absence of ethanol is less photosensitive as the observed ΔA_0 value of 0.009 is a fraction (<10%) of the static absorbance at 450 nm. This can be most simply explained by a relatively stronger heme−CO bond in P450 2E1. Another possible explanation is that newly photodissociated CO in the P450 2E1 has a high rate of geminate recombination whereby a large fraction of CO molecules never leave the active site, perhaps trapped in a site near the heme, and rebind more rapidly than our detection system can measure. Ethanol increased ΔA_0 (Figure 4), and thus increases the photodissociation efficiency. This ethanol effect may originate directly via an interaction with the heme−CO bond, or through mediating conformational changes in the heme region which facilitate CO egress.

Figure 4 also shows that the ethanol concentration dependencies of k and ΔA_0 differ, as the rate decrease is more responsive to ethanol than the increase in the rate of photodissociation. This shows that rate, which reflects conformational flexibility, is more sensitive to ethanol than factors which influence the heme−CO bond in the active site. Ethanol thus has a dual effect on P450 conformation and dynamics.

Effects of Other Substrates on the Kinetics of CO Binding to P450 2E1. The effects of several other P450 2E1 ligands were also evaluated. The kinetics in all cases were again monoexponential and yielded the kinetic parameters shown in Table 1. Isoniazid and acetaminophen both moderately reduced the CO binding rate while having no significant effects on ΔA_0. Pyrazole had no effect on either k or ΔA_0. Halothane and arachidonic acid had the most pronounced effects. Halothane greatly enhanced the photosensitivity of the heme−CO bond and markedly slowed the binding kinetics. The rate reduction by halothane (6.7 s^{-1}) is even more pronounced than that seen with 400 mM ethanol (136 s^{-1}). Arachidonic acid completely abolished photodissociation, and therefore, no kinetic data are presented in Table 1. This is an interesting observation in that the long-chain arachidonic acid has the most distinct structure of the tested compounds.

In light of ethanol being implicated as a substrate, inducer, and stabilizer of P450 2E1 as well as the effect of ethanol on drug metabolism, we investigated how ethanol affected P450 conformational dynamics in the presence of the other substrates. Figure 5A shows that ethanol generally reduced the CO binding rate to a comparable degree in the absence and presence of substrates. The exceptions were halothane and arachidonic acid. Ethanol had no effect on the already greatly decelerated CO binding rate caused by halothane alone. In the case of arachidonic acid, addition of ethanol restored photosensitivity (Figure 5B) and resulted in a binding rate similar to that of ethanol alone (Figure 5A). Ethanol did not significantly change the photosensitivity in the presence of the other substrates (Figure 5B).

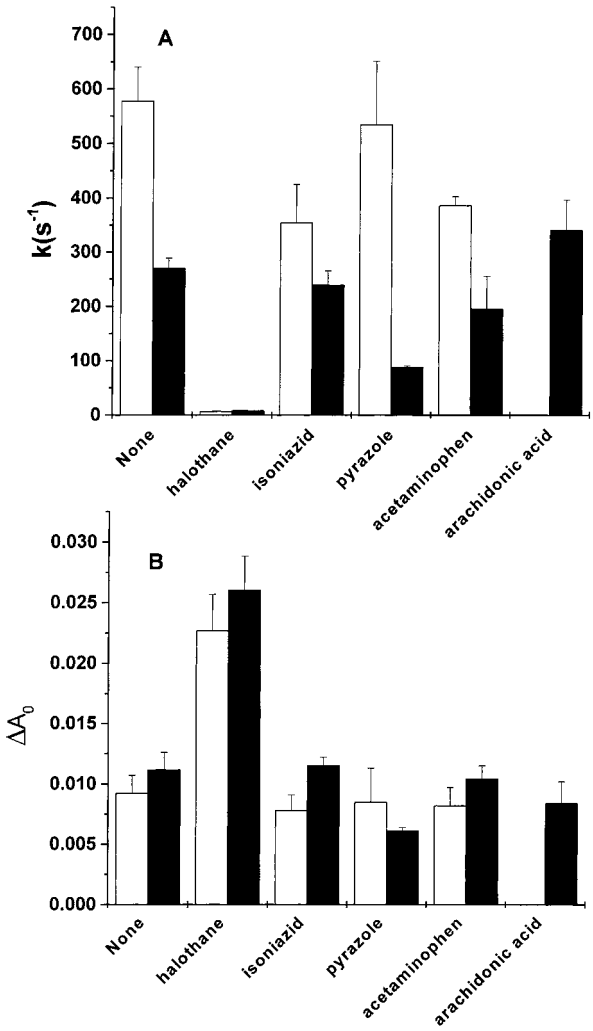

FIGURE 5: Effect of substrates and ethanol on the CO binding kinetic parameters of P450 2E1. (A) CO binding rates of P450 2E1. (B) CO photodissociation from P450 2E1. The effects of P450 2E1 substrates in the absence (white bars) and presence (black bars) of 50 mM ethanol are shown. Substrate concentrations were 1 mM, except for that of ethanol which was 50 mM. In panel A, no data are shown for arachidonic acid in the absence of ethanol, since photodissociation was not observed.

Molecular Modeling of the P450 2E1 Interaction with Arachidonic Acid. The unique results with halothane and arachidonic acid were interpreted with a structural model of P450 2E1. On the basis of its type I difference spectrum (Figure 2 and Table 1), halothane binds to P450 2E1 and displaces water as the axial ligand but does not bind to the heme. Its modulation of CO binding to P450 2E1 is not affected by ethanol, which implies that ethanol does not displace halothane from the active site. Arachidonic acid had no measurable difference spectrum, implying that it did not displace the water ligand from the heme. Yet its binding to the active site is evidenced by both its metabolism by P450 2E1 and the complete abolishment of photodissociation (Table 1 and Figure 5B). The combination of ethanol with arachidonic acid restored the kinetic parameters to those observed for ethanol alone (Figure 5A), implying that ethanol most likely displaced arachidonic acid from the active site.

On the basis of these observations, we conclude that the active site of P450 2E1 can accommodate both arachidonic acid and a liganded water molecule. To visualize this, we

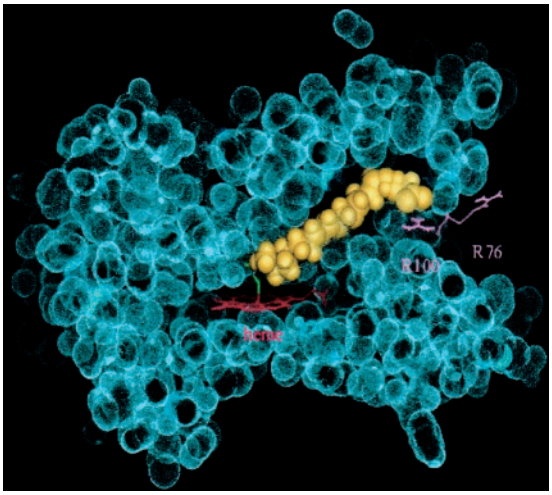

FIGURE 6: Model of the P450 2E1 complex with arachidonic acid. A slice view of a P450 model is presented to show binding of arachidonic acid (yellow) in its binding site. The heme group (red) and a CO molecule (green) are also shown. Two surface arginines (positions 76 and 100) are shown which engage in electrostatic contacts with the arachidonic acid carboxylate.

generated a model of P450 2E1 using techniques similar to those used previously for homology modeling of P450s 2B1 (*31*) and 1A2 (*32*). The model structure (Figure 6) has several features that can account for the experimental results. Arachidonic acid is shown binding along an elongated hydrophobic pocket with two basic amino acids (R76 and R100) near the surface to anchor its negatively charged carboxyl end. Between the distal end of arachidonic acid and the heme group, there is enough space for occupation by several water molecules. Thus, arachidonic acid binding would not displace water, consistent with the absence of a spin shift (Figure 2). This long pocket provides a rather large arachidonic acid−P450 interaction surface which would limit motions of quite a few residues in P450 2E1. This could potentially block the escape of photodissociated CO from the protein's interior, which is consistent with the suppression of photodissociation by arachidonic acid. The restoration of photodissociation when ethanol is present along with arachidonic acid (Figure 5B) suggests that ethanol inhibits arachidonic acid binding to the hydrophobic pocket.

DISCUSSION

Previous work in our laboratory using the flash photolysis technique has demonstrated the presence of alternate conformational substates within the P450 population whose rates of CO binding can be selectively modulated (inhibited or accelerated) by specific P450 substrates (*12*). This is most readily reflected by the multiexponential nature of the kinetic profiles. The identification of kinetically distinguishable conformers has helped explain some of the complexities in the kinetics of CO binding to P450s in the presence and absence of substrates. In this study, we found that P450 2E1 is different from the other P450s in that a single exponential describes the kinetics in both the absence and presence of substrates and inducers. The simple kinetics of P450 2E1 contrast with our previous findings that P450s 3A4 (*8*) and 1A1 (*10*) consist of multiple kinetically distinct species, and indicate that the population of P450 2E1 molecules is more homogeneous than the aforementioned P450s. This may not be too surprising, however, in view of the more limited range of substrate recognition by P450 2E1 relative to these other P450s, since most substrates are small hydrophobic molecules (e.g., benzene) or fatty acids (e.g., arachidonic acid). When interpreted in terms of a multiconformer model, the results imply that for some P450s (e.g., 3A4), a subset of the population can be modulated by a substrate or other effector while for P450 2E1 the whole population is affected.

The finding that ethanol reduced the CO binding rate and hence the dynamic fluctuations of P450 2E1 may relate to its previously reported properties. Although substrate stabilization of this P450 has been reported (*24*, *36*), its molecular mechanism is unknown. However, the ethanol-induced decrease in flexibility is quite consistent with greater stability, as lower flexibility tends to decrease a protein's susceptibility to proteolytic degradation (*37*). Although the ethanol effect is most directly derived from its binding to the active site and possibly other interior regions, one must also consider the possibility that ethanol exerts some effect on the lipid bilayer that is transmitted to the P450. However, the lack of an ethanol effect on P450 3A4 (Figure 3) suggests that the effect is P450 2E1 specific and does not originate from a general membrane perturbation.

We surveyed several substrates and inducers of P450 2E1 to determine their effects on the conformational dynamics. The results obtained with ethanol, halothane, and arachidonic acid were interpreted using a model which accounts for their effects on CO flash photolysis and difference spectra. The model has a long hydrophobic pocket that can accommodate arachidonic acid binding, a feature also found in a previously proposed P450 2E1 model (*38*). Our model has basic residues (arginines 76 and 100) at the surface of the pocket that can stabilize the negatively charged carboxyl group of the fatty acid. As this hydrophobic pocket may define a ligand access channel to the heme, its occupancy by substrate can block egress of CO ligand to the solvent. This is borne out by the lack of photodissociation in the presence of arachidonic acid. Other small, hydrophobic molecules such as halothane and ethanol can also bind along this pocket and disrupt hydrophobic interactions with substrates. This was seen as ethanol reversed the abatement of photodissociation caused by arachidonic acid by either displacing or repositioning the arachidonic acid so that CO egress was possible. Ethanol, however, did not affect modulation of P450 2E1 structural dynamics by halothane. This suggests that small, hydrophobic molecules such as halothane with high affinities or that bind by slightly different mechanisms (Table 1) can still fill the pocket. In the generation of our model, coordinates for water molecules were not assigned because of the inherent inaccuracy in their placement. However, our model for P450 2E1 has sufficient room for several molecules of water near the heme when arachidonic acid is bound to the pocket. This is consistent with our finding that arachidonic acid did not induce the difference spectrum typically observed when a substrate displaces the water ligand. A similar finding was reported for a P450 BM-3 mutant that metabolizes arachidonic acid, yet a typical substrate-induced spectral change was not observed (*39*).

The absence of a crystal structure determination for membrane-bound human cytochrome P450s makes it difficult to make inferences about the structural basis of the mechanisms controlling the P450−substrate interactions. The most

logical approach is to combine results about binding modes and P450−ligand interactions inferred from biophysical and biochemical characterization of the P450 with molecular modeling approaches. We thus combined static methods (difference spectroscopy), dynamic methods (flash photolysis), and theoretical modeling methods to gain insights into P450 2E1 structure and function, especially relating to the important questions of substrate stabilization and ethanol−drug interactions.

REFERENCES

1. Lu, A. Y., and West, S. B. (1979) *Pharmacol. Rev. 31*, 277−295.
2. Ryan, D. E., and Levin, W. (1990) *Pharmacol. Ther. 45*, 153−239.
3. Ortiz de Montellano, P. (1995) *Cytochrome P450 Structure, Mechanism, and Biochemistry*, Plenum Press, New York.
4. Nelson, D. R., Koymans, L., Kamataki, T., Stegeman, J. J., Feyereisen, R., Waxman, D. J., Waterman, M. R., Gotoh, O., Coon, M. J., Estabrook, R. W., Gunsalus, I. C., and Nebert, D. W. (1996) *Pharmacogenetics 6*, 1−42.
5. Ioannides, C. (1996) *Cytochromes P450: Metabolic and Toxicological Aspects*, CRC Press, Boca Raton, FL.
6. Gibson, G. G., Cinti, D. L., Sligar, S. G., and Schenkman, J. B. (1980) *J. Biol. Chem. 255*, 1867−1873.
7. Omata, Y., and Friedman, F. K. (1991) *Biochem. Pharmacol. 42*, 97−101.
8. Koley, A. P., Buters, J. T., Robinson, R. C., Markowitz, A., and Friedman, F. K. (1995) *J. Biol. Chem. 270*, 5014−5018.
9. Koley, A. P., Buters, J. T. M., Robinson, R. C., Markowitz, A., and Friedman, F. K. (1997) *J. Biol. Chem. 272*, 3149−3152.
10. Koley, A. P., Buters, J. T. M., Robinson, R. C., Markowitz, A., and Friedman, F. K. (1996) *Arch. Biochem. Biophys. 336*, 261−267.
11. Koley, A. P., Dai, R., Robinson, R. C., Markowitz, A., and Friedman, F. K. (1997) *Biochemistry 36*, 3237−3241.
12. Koley, A. P., Robinson, R. C., and Friedman, F. K. (1996) *Biochimie 78*, 706−713.
13. Koley, A. P., Robinson, R. C., Markowitz, A., and Friedman, F. K. (1997) *Biochem. Pharmacol. 53*, 455−460.
14. Koley, A. P., Robinson, R. C., Markowitz, A., and Friedman, F. K. (1995) *Biochemistry 34*, 1942−1947.
15. Koley, A. P., Robinson, R. C., Markowitz, A., and Friedman, F. K. (1994) *Biochemistry 33*, 2484−2489.
16. Fraser, A. G. (1997) *Clin. Pharmacokinet. 33*, 79−90.
17. Goasduff, T., and Cederbaum, A. I. (1999) *Arch. Biochem. Biophys. 370*, 258−270.
18. Lieber, C. S. (1997) *Clin. Chim. Acta 257*, 59−84.
19. Song, B. J. (1996) *Alcohol.: Clin. Exp. Res. 20*, 138A−146A.
20. Ronis, M. J., Lindros, K. O., and Ingelman-Sundberg, M. (1996) in *Cytochromes P450: Metabolic and Toxicological Aspects* (Ioannides, C., Ed.) pp 211−239, CRC Press, Boca Raton, FL.
21. Lee, S. S., Buters, J. T., Pineau, T., Fernandez-Salguero, P., and Gonzalez, F. J. (1996) *J. Biol. Chem. 271*, 12063−12067.
22. Laethem, R. M., Balazy, M., Falck, J. R., Laethem, C. L., and Koop, D. R. (1993) *J. Biol. Chem. 268*, 12912−12918.
23. Bell, L. C., and Guengerich, F. P. (1997) *J. Biol. Chem. 272*, 29643−29651.
24. Zhukov, A., and Ingelman-Sundberg, M. (1997) *Eur. J. Biochem. 247*, 37−43.
25. Grogan, J., Shou, M., Andrusiak, E. A., Tamura, S., Buters, J. T., Gonzalez, F. J., and Korzekwa, K. R. (1995) *Biochem. Pharmacol. 50*, 1509−1515.
26. Omura, T., and Sato, R. (1964) *J. Biol. Chem. 239*, 2379−2385.
27. Smith, P. K., Krohn, R. I., Hermanson, G. T., Mallia, A. K., Gartner, F. H., Provenzano, M. D., Fujimoto, E. K., Goeke, N. M., Olson, B. J., and Klenk, D. C. (1985) *Anal. Biochem. 150*, 76−85.
28. Leach, S. J., and Scheraga, H. A. (1960) *J. Am. Chem. Soc. 82*, 4790−4792.
29. Markowitz, A., Robinson, R. C., Omata, Y., and Friedman, F. K. (1992) *Anal. Instrum. (N.Y.) 20*, 213−221.
30. Ravichandran, K. G., Boddupalli, S. S., Hasermann, C. A., Peterson, J. A., and Deisenhofer, J. (1993) *Science 261*, 731−736.
31. Dai, R., Pincus, M. R., and Friedman, F. K. (1998) *J. Protein Chem. 17*, 121−129.
32. Dai, R., Zhai, S., Wei, X., Pincus, M. R., Vestal, R. E., and Friedman, F. K. (1998) *J. Protein Chem. 17*, 643−650.
33. Li, H., and Poulos, T. L. (1997) *Nat. Struct. Biol. 4*, 140−146.
34. Jefcoate, C. R. (1978) *Methods Enzymol. 52*, 258−279.
35. Chen, W., Peter, R. M., McArdle, S., Thummel, K. E., Sigle, R. O., and Nelson, S. D. (1996) *Arch. Biochem. Biophys. 335*, 123−130.
36. Roberts, B. J., Song, B. J., Soh, Y., Park, S. S., and Shoaf, S. E. (1995) *J. Biol. Chem. 270*, 29632−29635.
37. Fontana, A., Fassina, G., Vita, C., Dalzoppo, D., Zamai, M., and Zambonin, M. (1986) *Biochemistry 25*, 1847−1851.
38. Wang, M. H., Wade, D., Chen, L., White, S., and Yang, C. S. (1995) *Arch. Biochem. Biophys. 317*, 299−304.
39. Graham-Lorence, S., Truan, G., Peterson, J. A., Falk, J. R., Wei, S., Helvig, C., and Capdevila, J. H. (1997) *J. Biol. Chem. 272*, 1127−1135.

BI000129L